

Crystal structure of the Psb27 assembly factor at 1.6 Å: implications for binding to Photosystem II

Franck Michoux · Kenji Takasaka ·
Marko Boehm · Josef Komenda · Peter J. Nixon ·
James W. Murray

Received: 16 September 2011 / Accepted: 26 November 2011 / Published online: 23 December 2011
© Springer Science+Business Media B.V. 2011

Abstract The biogenesis and oxygen-evolving activity of cyanobacterial Photosystem II (PSII) is dependent on a number of accessory proteins not found in the crystallised dimeric complex. These include Psb27, a small lipoprotein attached to the lumenal side of PSII, which has been assigned a role in regulating the assembly of the Mn₄Ca cluster catalysing water oxidation. To gain a better understanding of Psb27, we have determined in this study the crystal structure of the soluble domain of Psb27 from *Thermosynechococcus elongatus* to a resolution of 1.6 Å. The structure is a four-helix bundle, similar to the recently published solution structures of Psb27 from *Synechocystis* PCC 6803 obtained by nuclear magnetic resonance (NMR) spectroscopy. Importantly, the crystal structure presented

here helps us resolve the differences between the NMR-derived structural models. Potential binding sites for Psb27 within PSII are discussed in light of recent biochemical data in the literature.

Keywords Monomeric and dimeric photosystem II · Assembly · Repair · Psb27 · Crystal structure · NMR · Docking

Abbreviations

D1	Photosystem II reaction centre subunit encoded by <i>psbA</i>
D2	Photosystem II reaction centre subunit encoded by <i>psbD</i>
CP43 and CP47	Photosystem II proximal light-harvesting subunits encoded by <i>psbC</i> and <i>psbB</i> , respectively
PsbO	Photosystem II manganese-stabilising polypeptide
PsbV	Cytochrome <i>c</i> -550
PsbU	Photosystem II 12-kDa extrinsic protein
RC47	Photosystem II complex lacking CP43
RCC1	Monomeric photosystem II
RCC2	Dimeric photosystem II
RMSD	Root mean square deviation

Electronic supplementary material The online version of this article (doi:10.1007/s11120-011-9712-7) contains supplementary material, which is available to authorized users.

F. Michoux (✉) · K. Takasaka · M. Boehm ·
P. J. Nixon · J. W. Murray
Division of Molecular Biosciences, Imperial College London,
Wolfson Biochemistry Building, South Kensington Campus,
London SW7 2AZ, UK
e-mail: franck.michoux@imperial.ac.uk

Present Address:

K. Takasaka
Division of Bioscience, Faculty of Science, Okayama
University, Okayama 700-8530, Japan

Present Address:

M. Boehm
National Renewable Energy Laboratory, 16253 Denver West
Parkway, FTLB-(190-04B), Golden, CO 80401, USA

J. Komenda
Institute of Microbiology, Academy of Sciences, 379 81 Třeboň,
Czech Republic

Introduction

The Photosystem II (PSII) complex functions as the light-driven water:plastoquinone oxidoreductase of oxygenic photosynthesis and is found in the thylakoid membranes of cyanobacteria and chloroplasts. The structure of dimeric PSII has been determined by X-ray crystallography for the cyanobacteria *Thermosynechococcus elongatus* (Ferreira

et al. 2004; Loll et al. 2005; Guskov et al. 2009) and *Thermosynechococcus vulcanus* (Kamiya and Shen 2003; Umena et al. 2011). In the case of *T. elongatus*, each monomer is composed of 17 intrinsic and 3 extrinsic subunits and a variety of co-factors. The way in which PSII is assembled from its component parts is still largely unknown. Several PSII sub-complexes have been identified and characterised in cyanobacterial membranes, which has allowed us to propose detailed models for the assembly of PSII (Nixon et al. 2010). Recent ideas suggest that monomeric PSII complexes are assembled from smaller sub-complexes (Boehm et al. 2011). First, a PSII reaction centre (PSII RC) complex is formed from PsbI-precursor D1 (Dobakova et al. 2007) and cytochrome *b*₅₅₉-D2 (Komenda et al. 2004) sub-complexes. A CP47 complex is then attached to create the RC47 complex, after which the CP43 complex is added to form non-oxygen-evolving monomeric PSII complex. At this stage the oxygen-evolving Mn₄Ca cluster is assembled, the luminal extrinsic proteins are attached and PSII can dimerise.

The PSII complex is prone to light-induced damage, often termed photoinhibition (Adir et al. 2003). Damaged subunits, predominantly the D1 subunit, are replaced in the so-called ‘PSII repair cycle’. Current models suggest that the damaged PSII complex partially disassembles to the form the monomeric RC47 complex (Komenda et al. 2004), and the damaged D1 protein is degraded by an FtsH protease complex (Barker et al. 2006) and replaced by a newly synthesised copy of D1. Oxygen-evolving monomeric and dimeric complexes are then reformed as in PSII assembly.

A number of accessory factors have recently been identified in cyanobacteria with possible roles in the assembly of PSII but which are absent in the PSII holoenzyme (reviewed in Nixon et al. 2010). These include the Psb27 subunit which is predicted to be targeted to the thylakoid lumen and which was originally identified in PSII preparations isolated from *Synechocystis* sp. PCC 6803 (hereafter *Synechocystis* 6803) by

Ikeuchi et al. (1995) and later by Kashino et al. (2002). Subsequently, non-oxygen-evolving PSII monomeric complexes were isolated containing Psb27 but lacking the extrinsic PsbO, PsbU and PsbV proteins (Nowaczyk et al. 2006; Mamedov et al. 2007). Mutant studies support the idea that Psb27 is involved in regulating the assembly of the Mn₄Ca cluster (Nowaczyk et al. 2006; Roose and Pakrasi 2008). However, the binding site of Psb27 in PSII is currently unknown.

Psb27 is present in all known oxygenic phototrophs except *Gloeobacter violaceus*. Analysis of the cyanobacterial phylogenetic tree in (Gupta 2009) would suggest that Psb27 was present in the last common ancestor of cyanobacteria, and has been lost in *Gloeobacter*. In most cyanobacteria, Psb27 is thought to be a lipoprotein (Nowaczyk et al. 2006); however, in *Prochlorococcus* sp, *Synechococcus* JA-3-3ab and *Synechococcus* JA-3-3B'a2, the predicted lipobox sequence is absent. Two Psb27 homologues are found in *Arabidopsis thaliana* chloroplasts (Fig. 1), neither of which appears to be a lipoprotein, in common with other higher plant Psb27 sequences (Chen et al. 2006; Wei et al. 2010).

To gain a better understanding of the molecular function of Psb27, two groups have independently proposed 3D structural models of the Psb27 protein from *Synechocystis* 6803 using nuclear magnetic resonance (NMR) spectroscopy methods (Cormann et al. 2009; Mabbitt et al. 2009). In both cases, Psb27 was revealed to be a four-helix bundle; however, there are significant differences in the two structural models which complicate attempts to determine the potential binding site of Psb27 in PSII using in silico docking approaches. While Cormann et al. (2009) located the Psb27 protein in proximity to CP47, Mabbitt et al. (2009) placed it on the other side of the complex, next to CP43.

In this article, we report the 3D crystal structure of the soluble domain of Psb27 from *T. elongatus* to a resolution of 1.6 Å. Our structure confirms that Psb27 is a four-helix bundle in *T. elongatus* and has helped us

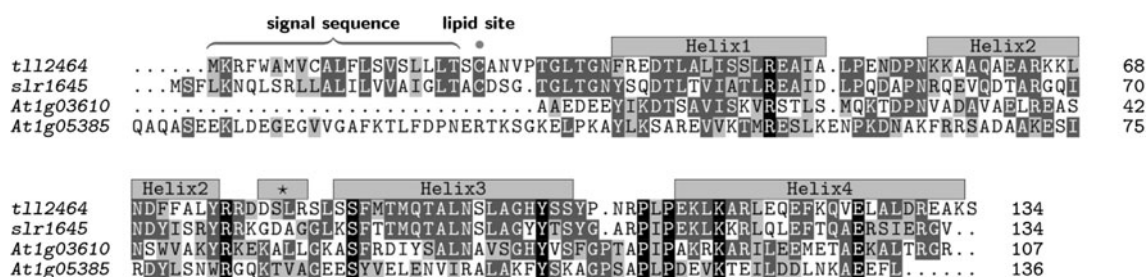


Fig. 1 Amino acid comparison between Psb27 from *Synechocystis* 6803 and *T. elongatus*. Alignment of the Psb27 from *T. elongatus* (t112464) versus that from *Synechocystis* 6803 (slr1645) and the two homologues found in *Arabidopsis* (At1g05385 for LPA19 and At1g03600). The alignment was computed using ClustalX

(Thompson et al. 1997), and rendered with TeXshade (Beitz 2000). Identical residues are in black; similar residues in grey. The transit sequences and lipided cysteines in cyanobacteria are marked. The four main helices and helix * are indicated with grey boxes

resolve differences in the NMR-derived structural models to allow a reassessment of the potential binding site within PSII.

Materials and methods

Thermosynechococcus elongatus BP1 strain

The wild-type *T. elongatus* strain was obtained from Prof. James Barber (Imperial College London, UK).

Psb27 construct generation

The DNA sequence corresponding to the Psb27 homologue of *T. elongatus* (tll2464) without its predicted signal peptide and the sequence encoding the lipid-binding residue Cys²² was cloned into a pRSET-A vector modified to add a thrombin cleavage site (gifted by Dr Ernesto Cota, Imperial College London). The corresponding PCR fragment was amplified from *T. elongatus* genomic DNA using Phusion polymerase (NEB, UK) and primers Psb27-*Bam*HI-F (5'-TATATAGGATCCAATGTGCCTACGGGGCTAACGGGCAAT-3') and Psb27-*Hind*III-R (5'-TCTCTCAAGCTTTTACTAGGACTTCGCTTCGCGATCAAGGGCGAGT-3'), double digested by *Bam*HI/*Hind*III and ligated (Quick Ligation Kit, NEB, UK) into the modified and *Bam*HI/*Hind*III linearised pRSET-A. The vector was then transformed into KRX *Escherichia coli* cells (Promega, UK).

Expression, purification and crystallisation of Psb27

Expression of His₆-tagged Psb27 was induced by the addition of 2 g/l of rhamnose, and cells were grown at 18°C overnight. Cells were lysed with a sonicator (Sonics and Materials, CT, USA) in lysis buffer (50 mM Tris-HCl pH 7.9, 500 mM NaCl and 1 mM MgCl₂) supplemented with one Complete Protease Inhibitor Cocktail-EDTA Tablet (Roche, UK) per 50 ml lysis buffer. Broken cells were spun down for 10 min at 4°C at 18,000×g and the supernatant was mixed with a Ni-IDA resin (Generon, UK). Non-specifically bound proteins were removed by washing three times with wash buffer (20 mM Tris-HCl pH 7.9, 500 mM NaCl and 60 mM imidazole) and His₆-Psb27 was eluted with elution buffer (20 mM Tris-HCl pH 7.9, 500 mM NaCl and 1 M imidazole). Purified His₆-Psb27 was further dialysed overnight at 4°C in 20 mM Tris-HCl pH 7.9 and 200 mM NaCl. The His-tag present in the construct was removed by thrombin (GE Healthcare, UK) digestion at a ratio of 1 U of thrombin per 100 µg of purified Psb27. Proteolysis was performed overnight at 4°C, and the digested sample was reloaded onto a Ni-IDA column. The flow through containing Psb27 without the His-tag was

concentrated at 4°C to 26 mg/ml with a centrifugal concentrator device with a molecular weight cut off of 3.5 kDa (Sartorius, Germany). Protein was screened against sparse matrix screens using a Mosquito robot. Small crystals were seen fortuitously in a condition that had been improperly sealed, increasing the precipitant concentration. Custom screens against high concentrations of PEG were then performed. Crystals for structure solution were grown by hanging drop vapour diffusion with protein solutions at 26 mg/ml mixed with an equal volume of 35–40% PEG 4000. Crystals were cryoprotected in the mother-liquor solution with 30% (v/v) glycerol added, then flash-cooled in liquid nitrogen.

Protein structure determination

Data were integrated and scaled with XDS (Kabsch 2010) or MOSFLM (Leslie 1992) and programs of the CCP4 suite (1994). 5% of reflections were set aside as the free set for cross-validation. The first model in the PDB file 2KMF was truncated using Chainsaw MIXS mode (Stein 2008), and used as a model in PHASER (McCoy et al. 2007). A search was performed against a preliminary 1.9 Å resolution dataset. The top scored solution had a low translation Z-score (4.3) and log-likelihood gain (34). However, when this solution was refined in REFMAC the R_{free} dropped rapidly, indicating that it was correct (Table 1). The structure was refined against higher resolution data from another crystal in REFMAC (Murshudov et al. 1997) with cycles of manual model-building in COOT (Emsley et al. 2010).

Protein Data Bank accession code

The refined co-ordinates of the 3D model of Psb27 from *T. elongatus* have been deposited at the Protein Data Bank using the accession code 2Y6X.

Results and discussion

Expression and crystallisation of the Psb27 protein from *T. elongatus*

An N-terminal His₆-tagged derivative of Psb27 (tll2464 gene product) from *T. elongatus* was overexpressed in *E. coli*. The sequence corresponding to the N-terminal signal peptide and the lipidated cysteine of Psb27 (Nowaczyk et al. 2006) (Fig. 1) was replaced by a 6xHis tag and a thrombin recognition site LVPRGS. Sequence alignments between Psb27 from *T. elongatus* and from *Synechocystis* 6803 (used for NMR structure determination) revealed an amino-acid identity of 56% and a similarity of 75% (Fig. 1).

Table 1 Data collection and refinement statistics for the Psb27 crystal structure

	Lower resolution native	High resolution native
X-ray source	Soleil Proxima-1	Diamond I04
Data processing	XDS	Mosflm/Scala
Space group	$P2_12_12_1$	$P2_12_12_1$
Unit-cell parameters		$a = 36.930 \text{ \AA}$, $b = 50.820 \text{ \AA}$, $c = 53.070 \text{ \AA}$, $\alpha = \beta = \gamma = 90$
Wavelength (\AA)	1.12713	1.28310
Resolution (\AA)	45–1.94 (2.06–1.94)	30.3–1.6 (1.69–1.60)
Measured reflections	34,838 (5,473)	196,836 (12,971)
Unique reflections	7,694 (1,191)	13,705 (1,963)
Mn(I/sd)	10.47 (2.78)	15.9 (3.16)
Completeness (%)	98.7 (97.2)	99.8 (100.0)
Multiplicity	4.53 (4.60)	6.52 (6.61)
Rmeas (%)	0.13 (0.79)	0.07 (0.63)
Solvent content (%)		39%
$R_{\text{work}}/R_{\text{free}}$ (%)		19.0/23.8
Protein atoms		894
Solvent atoms		131
RMSD from ideal		
Bond lengths (\AA)		0.023
Bond angles ($^\circ$)		1.892
Average B factor (\AA^2)		16.8
Ramachandran favoured region (%)		100
Ramachandran allowed region (%)		0

$$R_{\text{meas}} = \frac{\sum(h) [\text{Sqrt}(n/(n-1)) \sum(j) [I(hj)]]}{\sum(j) [I(hj)]}$$

5% reflections in R_{free}

Soluble His₆-Psb27 was purified to near homogeneity by immobilized metal ion affinity chromatography (IMAC). After elution of His₆-Psb27 from the Ni²⁺-charged column, a single band migrating at about 15 kDa was detected by Coomassie staining, corresponding to the molecular mass of His₆-Psb27 (Online Resource Fig. S1.a). The His-tag was removed by thrombin cleavage (Online Resource Fig. S1.b) and Psb27 was re-purified and concentrated to 26 mg/ml. After cleavage, the predicted N-terminus of expressed Psb27 started with the amino-acid sequence GSANVP, the amino acids glycine and serine derived from the thrombin cleavage site. Crystallisation screenings were performed using hanging drop plates, resulting in the formation of crystals in high concentrations (35–40%) of PEG 4000 (Online Resource Fig. S2).

3D crystal structure of Psb27

Native datasets were obtained at a resolution of 1.6 \AA , and a molecular replacement using each model structure of Psb27 from *Synechocystis* 6803 (PDB: 2KMF and 2KND) was attempted. Only molecular replacement using 2KMF (Mabbitt et al. 2009) allowed the solution of the 3D structure of Psb27 from *T. elongatus* (Fig. 2). This 3D

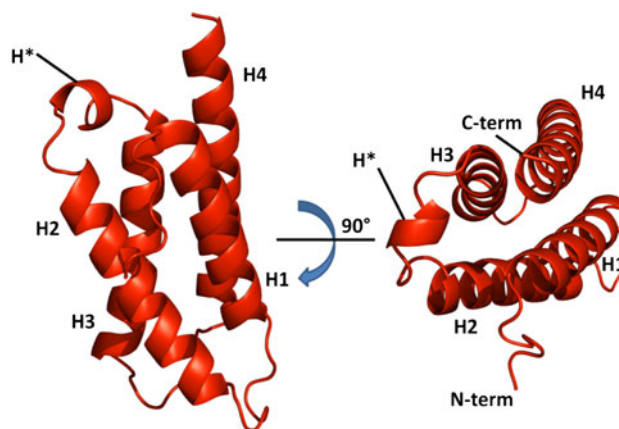


Fig. 2 Crystal structure of Psb27 from *T. elongatus* 3D structure of Psb27 from *T. elongatus* (PDB 2Y6X) obtained by molecular replacement and visualised using PyMol (DeLano 2002). Alpha helices are indicated as H1–H4 and H*

structure has four helices arranged in a right-handed up-down-up-down fold (H1–H4), as well as a small helix between H2 and H3 (designated H*), and a less-ordered N-terminus, where the lipocysteine is located in native Psb27. The N-terminal residues, GSANV, were not visible

in the crystal structure; the first amino acid that could be identified was the proline residue at position 26 in the precursor Psb27 sequence.

Comparison of Psb27 structures

Our 1.6 Å resolution structure was compared to the previously published NMR structures for Psb27 from *Synechocystis* 6803 and was found to have a more compact and folded 3D structure. The denser nature of a protein crystal could explain the more compact and defined shape of Psb27 from *T. elongatus* as compared to the more flexible structures obtained by NMR of Psb27 from *Synechocystis* 6803.

A more detailed analysis of the backbone structures (Fig. 3a) and the surface charges (Fig. 3b) led to the identification of several differences with previously published Psb27 NMR structures. Based on a comparison of the Psb27 backbones (Fig. 3a), the overall structure of Psb27 from *T. elongatus* appears to be more similar to the 2KMF NMR structure of Psb27 from *Synechocystis* 6803, with average distances measured between these two superimposed 3D models (RMSD) reaching only 1.8 Å, whereas the same parameters led to a value of 4.1 Å for 2KND. Furthermore, the surface charges seem to have a better correlation between Psb27 from *T. elongatus* and the 2KMF structure of *Synechocystis* 6803 (Fig. 3b).

Of particular interest are the surface charges located on helices H3 and H4, which were previously described as being the potential binding region of Psb27 to PSII

(Cormann et al. 2009). In the crystal structure and in the 2KMF NMR structure, the H3 helix does not have a global positive charge as compared to helix H4 (Fig. 3b), most likely due to the residue glutamate 98 (Glu⁹⁸), numbered accordingly to the annotation of both NMR structures. This residue, which corresponds to the glutamate residue at position 119 in *T. elongatus* and position 121 in *Synechocystis* 6803, seems to be buried in the 2KND structure. Moreover, helices 1 and 2 are largely out of register in structure 2KND.

From these discrepancies, it would appear that the binding region of Psb27 cannot be predicted using the 2KND NMR structure, raising doubts on the validity of the recently published docking model, which localised Psb27 in the vicinity of CP47 and D2 (Cormann et al. 2009).

In silico localisation of Psb27 on the luminal side of PSII

The Psb27-binding site in PSII is currently unknown. However, candidate sites can be suggested on the basis of in silico docking experiments coupled with the currently available biochemical data. Docking of *T. elongatus* Psb27 against the PSII structure of *T. elongatus* (PDB code 3BZ1) with extrinsic proteins removed was performed using the Hex docking server (Macindoe et al. 2010). Docking solutions not on the luminal side of the membrane were rejected as implausible based on prior knowledge. Of the rest, the best ten docking solutions clustered around the

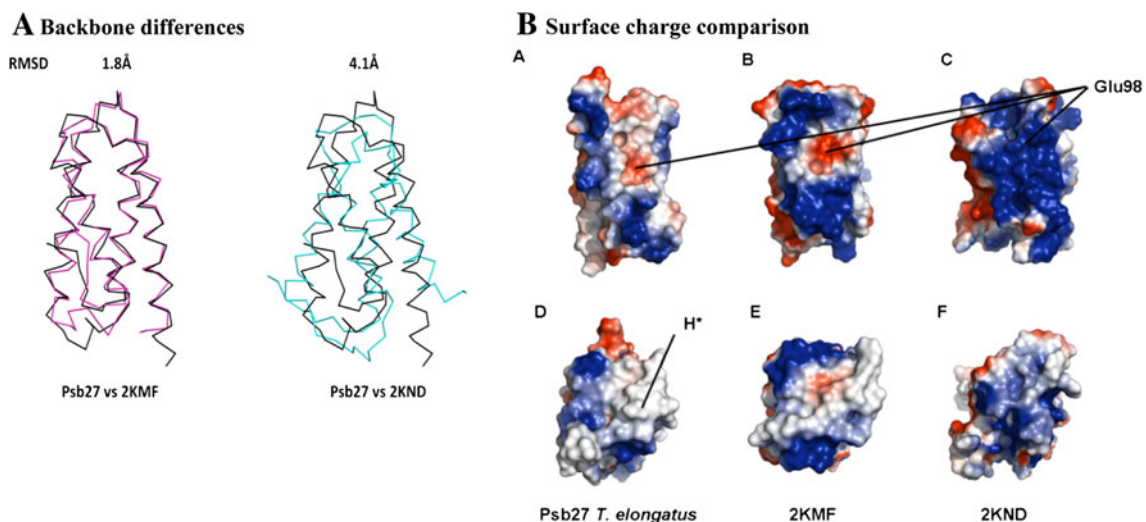


Fig. 3 Comparison between our Psb27 structure and previously published NMR structures of Psb27. **a** The previously published backbones were compared using the root mean square deviation (RMSD), as indicated, when superposing each *Synechocystis* 6803 Psb27 (2KMF, pink and 2KND, cyan) onto *T. elongatus* Psb27 (black) respectively. **b** The surface charges of each Psb27 protein are

visualised from the H3–H4 side (*top*) and H* side (*bottom*) views. The potential location of the amino acid glutamate 98 (numbered as in both NMR structures) is indicated. The colour code representing the surface charges are blue for positive charges, red for negative charges. All figures were created using Pymol (deLano 2002)

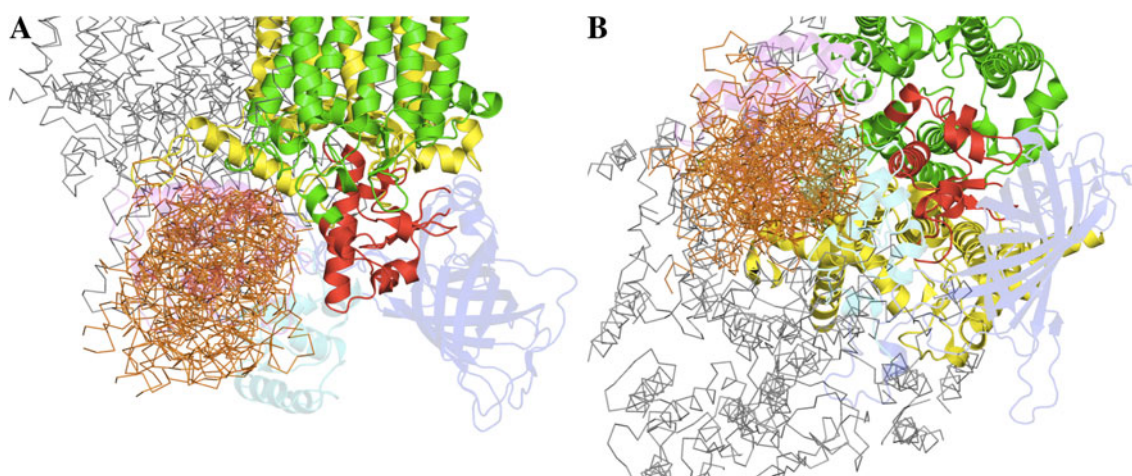


Fig. 4 Localisation of Psb27 on the luminal side of PSII in *T. elongatus*. Best 10 docking solutions of Psb27 against PSII (PDB: 3BZ1) on the luminal side of the complex view from the *side* (a) and from the *bottom* (b). Psb27 backbones are shown in orange, PsbO in

blue, D1 in yellow, PsbV in magenta, PsbU in cyan and CP43 in green. The loop of CP43 susceptible to proteolysis *in vivo* is indicated in red (Komenda et al. 2011)

PsbV-binding site, as shown in Fig. 4, in line with an earlier suggestion (Mabbitt et al. 2009). Such a location for Psb27 binding in PSII is consistent with recent studies showing that Psb27 co-purifies with the unassembled CP43 complex, that the large luminal loop of CP43 connecting the fifth and sixth transmembrane helices is sensitive to proteolytic cleavage *in vivo* in the absence of Psb27 (Fig. 4, red section of CP43; Komenda et al. 2011) and that LPA19, a Psb27 homologue, recognises the C-terminal region of D1 in *Arabidopsis* (Wei et al. 2010). In addition, the docking solutions shown in Fig. 4 do not occupy the binding site for PsbO consistent with recent studies suggesting that PsbO, but not PsbV, is still able to bind to monomeric PSII complexes containing His-tagged Psb27 (Liu et al. 2011a). Other docking programmes have placed Psb27 closer to the PsbO-binding site but still on the CP43 side of the complex (Fagerlund and Eaton-Rye 2011). Recent chemical cross-linking experiments also support an association between CP43 and Psb27 (Liu et al. 2011b). One of the cross-linked sites in CP43, at residue CP43-Asp³²¹, lies in the predicted binding site for Psb27 shown in Fig. 4, whereas the second site, at CP43-Lys²¹⁵, is located much further away. However, it is not yet clear whether these cross-links occur between Psb27 and CP43 bound to the same monomeric PSII complex or reflect a non-physiological interaction between Psb27 and CP43 bound to two separate PSII complexes.

In conclusion, we have solved the crystal structure of the Psb27 protein from *T. elongatus*. *In silico* docking experiments and recent biochemical data suggest a possible binding site for Psb27 close to the PsbV-binding site in PSII. Future studies will need to test this possibility.

Acknowledgments The authors thank the staff of SOLEIL Light Source for their help. FM, MB and PJN would like to thank the BBSRC (BB/E006388/1) and Engineering and Physical Sciences Research Council (EPSRC, EP/F00270X/1), and JK to the Czech Science Foundation (GACR, P501/11/0377) and Algatech (CZ.1.05/2.1.00/03.0110) for the respective financial supports. JWM holds a Biotechnology and Biological Sciences Research Council (BBSRC) David Phillips Fellowship (BB/F023308/1).

References

- Adir N, Zer H, Shochat S, Ohad I (2003) Photoinhibition—a historical perspective. *Photosynth Res* 76:343–370
- Barker M, de Vries R, Nield J, Komenda J, Nixon PJ (2006) The deg proteases protect *Synechocystis* sp. PCC 6803 during heat and light stresses but are not essential for removal of damaged D1 protein during the photosystem two repair cycle. *J Biol Chem* 281:30347–30355
- Beitz E (2000) TEXshade: shading and labeling multiple sequence alignments using LaTeX2e. *Bioinformatics* 16:135–139
- Boehm M, Romero E, Reisinger V, Yu J, Komenda J, Eichacker LA, Dekker JP, Nixon PJ (2011) Investigating the early stages of Photosystem II assembly in *Synechocystis* sp. PCC 6803: isolation of CP47 and CP43 complexes. *J Biol Chem* 286:14812–14819
- CCP4 (1994) The CCP4 suite: programs for protein crystallography. *Acta Crystallogr* 50:760–763
- Chen H, Zhang D, Guo J, Wu H, Jin M, Lu Q, Lu C, Zhang L (2006) A Psb27 homologue in *Arabidopsis thaliana* is required for efficient repair of photodamaged photosystem II. *Plant Mol Biol* 61:567–575
- Cormann KU, Bangert JA, Ikeuchi M, Rogner M, Stoll R, Nowaczyk MM (2009) Structure of Psb27 in solution: implications for transient binding to photosystem II during biogenesis and repair. *Biochemistry* 48:8768–8770
- DeLano WL (2002) The PyMOL molecular graphics system. DeLano Scientific, San Carlos

- Dobakova M, Tichy M, Komenda J (2007) Role of the PsbI protein in photosystem II assembly and repair in the cyanobacterium *Synechocystis* sp. PCC 6803. *Plant Physiol* 145:1681–1691
- Emsley P, Lohkamp B, Scott WG, Cowtan K (2010) Features and development of Coot. *Acta Crystallogr* 66:486–501
- Fagerlund RD, Eaton-Rye JJ (2011) The lipoproteins of cyanobacterial photosystem II. *J Photochem Photobiol* 104:191–203
- Ferreira KN, Iverson TM, Maghlaoui K, Barber J, Iwata S (2004) Architecture of the photosynthetic oxygen-evolving center. *Science* 303:1831–1838
- Gupta RS (2009) Protein signatures (molecular synapomorphies) that are distinctive characteristics of the major cyanobacterial clades. *Int J Syst Evol Microbiol* 59:2510–2526
- Guskov A, Kern J, Gabdulkhakov A, Broser M, Zouni A, Saenger W (2009) Cyanobacterial photosystem II at 2.9-Å resolution and the role of quinones, lipids, channels and chloride. *Nat Struct Mol Biol* 16:334–342
- Ikeuchi M, Shukla VK, Pakrasi HB, Inoue Y (1995) Directed inactivation of the *psbI* gene does not affect photosystem II in the cyanobacterium *Synechocystis* sp. PCC 6803. *Mol Gen Genet* 249:622–628
- Kabsch W (2010) Xds. *Acta Crystallogr* 66:125–132
- Kamiya N, Shen JR (2003) Crystal structure of oxygen-evolving photosystem II from *Thermosynechococcus vulcanus* at 3.7-Å resolution. *Proc Natl Acad Sci USA* 100:98–103
- Kashino Y, Koike H, Yoshio M, Egashira H, Ikeuchi M, Pakrasi HB, Satoh K (2002) Low-molecular-mass polypeptide components of a photosystem II preparation from the thermophilic cyanobacterium *Thermosynechococcus vulcanus*. *Plant Cell Physiol* 43:1366–1373
- Komenda J, Reisinger V, Muller BC, Dobakova M, Granvogl B, Eichacker LA (2004) Accumulation of the D2 protein is a key regulatory step for assembly of the photosystem II reaction center complex in *Synechocystis* PCC 6803. *J Biol Chem* 279:48620–48629
- Komenda J, Knoppová J, Kopečná J, Sobotka R, Halada P, Yu J, Nickelsen J, Boehm M, Nixon PJ (2011) The Psb27 assembly factor binds to the CP43 complex of Photosystem II in the cyanobacterium *Synechocystis* sp. PCC 6803. *Plant Physiol*. doi:10.1104/pp.111.184184.
- Leslie AGW (1992) Recent changes to the MOSFLM package for processing film and image plate data. In: Joint CCP4 and ESF-EACBM newsletters on protein crystallography 26
- Liu H, Roose JL, Cameron JC, Pakrasi HB (2011a) A genetically tagged Psb27 protein allows purification of two consecutive PSII assembly intermediates in *Synechocystis* 6803, a cyanobacterium. *J Biol Chem* 286:24865–24871
- Liu H, Huang RY, Chen J, Gross ML, Pakrasi HB (2011b) Psb27, a transiently associated protein, binds to the chlorophyll binding protein CP43 in photosystem II assembly intermediates. *Proc Natl Acad Sci USA* 108:18536–18541
- Loll B, Kern J, Saenger W, Zouni A, Biesiadka J (2005) Towards complete cofactor arrangement in the 3.0 Å resolution structure of photosystem II. *Nature* 438:1040–1044
- Mabbitt PD, Rautureau GJ, Day CL, Wilbanks SM, Eaton-Rye JJ, Hinds MG (2009) Solution structure of Psb27 from cyanobacterial photosystem II. *Biochemistry* 48:8771–8773
- Macindoe G, Mavridis L, Venkatraman V, Devignes MD, Ritchie DW (2010) HexServer: an FFT-based protein docking server powered by graphics processors. *Nucleic Acids Res* 38:445–449
- Mamedov F, Nowaczyk MM, Thapper A, Rogner M, Styring S (2007) Functional characterization of monomeric photosystem II core preparations from *Thermosynechococcus elongatus* with or without the Psb27 protein. *Biochemistry* 46:5542–5551
- McCoy AJ, Grosse-Kunstleve RW, Adams PD, Winn MD, Storoni LC, Read RJ (2007) Phaser crystallographic software. *J Appl Crystallogr* 40:658–674
- Murshudov GN, Vagin AA, Dodson EJ (1997) Refinement of macromolecular structures by the maximum-likelihood method. *Acta Crystallogr* 53:240–255
- Nixon PJ, Michoux F, Yu J, Boehm M, Komenda J (2010) Recent advances in understanding the assembly and repair of photosystem II. *Ann Bot* 106:1–16
- Nowaczyk MM, Hebel R, Schlodder E, Meyer HE, Warscheid B, Rogner M (2006) Psb27, a cyanobacterial lipoprotein, is involved in the repair cycle of photosystem II. *Plant Cell* 18:3121–3131
- Roose JL, Pakrasi HB (2008) The Psb27 protein facilitates manganese cluster assembly in photosystem II. *J Biol Chem* 283:4044–4050
- Stein N (2008) CHAINSAW: a program for mutating pdb files used as templates in molecular replacement. *J Appl Crystallogr* 41:641–643
- Thompson JD, Gibson TJ, Plewniak F, Jeanmougin F, Higgins DG (1997) The CLUSTAL X windows interface: flexible strategies for multiple sequence alignment aided by quality analysis tools. *Nucleic Acids Res* 25:4876–4882
- Umena Y, Kawakami K, Shen JR, Kamiya N (2011) Crystal structure of oxygen-evolving photosystem II at a resolution of 1.9 Å. *Nature* 473:55–60
- Wei L, Guo J, Ouyang M, Sun X, Ma J, Chi W, Lu C, Zhang L (2010) LPA19, a Psb27 homolog in *Arabidopsis thaliana*, facilitates D1 protein precursor processing during PSII biogenesis. *J Biol Chem* 285:21391–21398